Latin American Journal of Solids and Structures
www.lajss.org

Progressive deformation behaviour of thin cylindrical shell under cyclic temperature variation using Combined Hardening Chaboche Model

Abstract

This study intends to evaluate thermal ratchetting deformation due to cyclic thermal loading along the axis of a smooth cylindrical shell. Two cases of progressive deformation behaviour are discussed for different loading methods. The aim of the first case is to recognize the shakedown behaviour of the cylinder under applied loading cycles. Alternatively, second case is highlighting the ratchetting behaviour of the cylinder. Based on the loading method in second case, a smooth thin hollow cylinder is considered to simulate the progressive deformation. This condition simulates the $1/25^{th}$ scale down model of the Prototype Fast Breeder Reactor (PFBR) main vessel.

Keywords

Thermal Ratchetting, Progressive deformation, Thermal gradient, Isotropic hardening, Kinematic hardening, Chaboche Model.

AshutoshMishra[a]
R. Suresh Kumar[b]
P. Chellapandi[c]

[a]Indira Gandhi Centre for Atomic Research, Kalpakkam, India.
ashutoshjssate@gmail.com
[b]Indira Gandhi Centre for Atomic Research, Kalpakkam.
[c]Indira Gandhi Centre for Atomic Research, Kalpakkam.

1 INTRODUCTION

Thermal ratchetting due to sodium free level variation is one of the critical phenomenon which is considered in the design of the reactor assembly of the PFBR. Thermal ratchetting can cause dimensional instability in the structure due to excessive deformation beyond allowable strain limits as per RCC-MR (1993) and ASME (1995). The free levels according to Figure 1 are hot pool level within an inner vessel, cold pool level between inner vessel and inner thermal baffle, restitution collector level between inner and outer thermal baffles, feeding collector level between outer thermal baffle and main vessel.

Sodium free level varies during normal operations and other operating conditions depending upon the temperatures of hot and cold pools. During normal operation, the upper cylindrical portion of the inner vessel (in the vicinity of hot pool sodium free level) is highly affected by level variations. Therefore, the wetting surface of the vessel experiences the temperature of sodium immediately without an appreciable film drop, because of the high heat transfer coefficient of sodium. On the contrary, heat transfer of coefficient of argon contact surface is low and the temperature is approximately equal to the mean value (337 °C) between hot pool surface temperature (547 °C) and

roof slab bottom temperature (127 °C). Thus the temperature difference of nearly 200 °C is the cause of developed thermal stresses which varies with position and time and results in thermal ratchetting or shakedown.

In this paper, thermal ratchetting behaviour of thin smooth cylindrical shell has been analyzed. Since ratchetting in austenitic stainless steel structure includes plastic straining with cyclic hardening property, it is essential to involve sophisticated constitutive model to simulate inelastic behaviour such as in Lemaitre and Chaboche (1990), Chaboche and Rousselier (1983). There are various literatures available on thermal ratchetting for high temperature reactor components as in Chaboche (1994), Chellapandi et al. (2000) and Igari et al. (2000). Chaboche combined isotropic and kinematic hardening model is implemented in user defined subroutine with semi-implicit integration technique for plasticity calculation. Transient thermal loading of 550 °C is achieved by FORTRAN coding programmed into ABAQUS FILM subroutine.

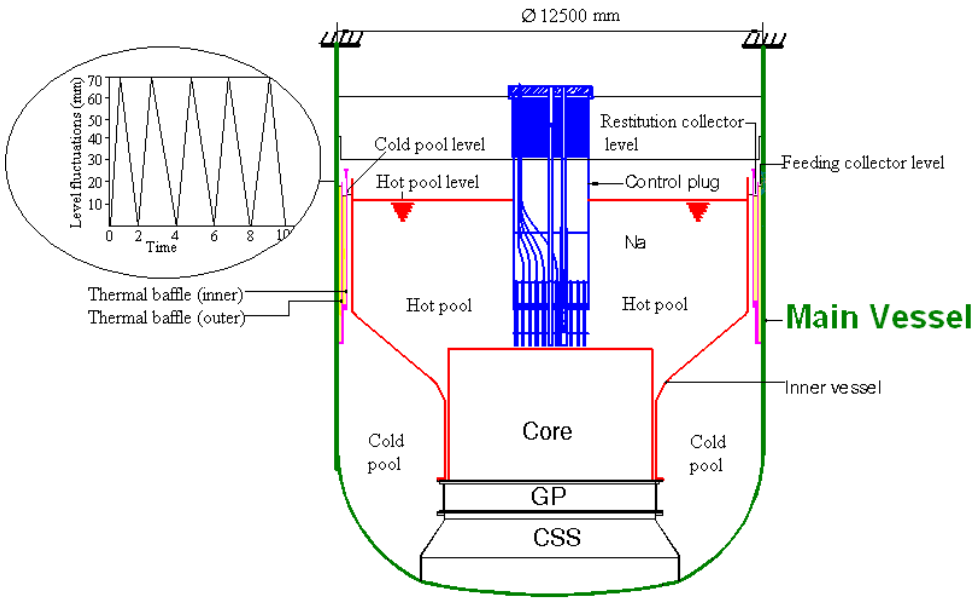

Figure 1: Typical sodium free level variations in main vessel of PFBR.

2 BACKGROUND TO RATCHETTING

Various literatures are available to evaluate ratchetting by design rules such as in ASME (1995), which is based on elastic core stress concept considering O'Donnell-Porowski diagram, and in RCC-MR (1993), which is based on effective stress concept considering Efficiency Index diagram. However, the ratchetting in a cylindrical shell subjected to cyclic axial thermal gradients with or without mechanical load is a special category with a general frame of thermal ratchetting which mainly the Sodium Cooled Fast Reactor (SFR) components experience at the vicinity of sodium free level. Robust design rules are not available in the design codes and realistic inelastic analysis is the only route. Classical ratchetting models, like in Bree (1967), discussed the evolution of ratchetting phe-

nomenon due to primary and secondary load combination. However, thermal ratchetting in reactor components can occur by secondary stresses alone. The ratchetting evaluation method in DDS (Demonstration Plant Design standard) discussed by Wada et al. (1997) was established and used for inelastic analysis for different combination of loads. Japanese LMR (Liquid Metal Reactor) design code of DDS (1998) implemented methods for evaluating ratchetting strain considering loading with several combinations of primary and secondary stresses with simultaneous imposition of secondary membrane and bending stresses. RCC-MR working group also presented the work on prediction of ratchetting considering the steady state assessment procedure for structures in European Fast Reactor (EFR). Comparative study of predictive methods for ratchetting was discussed by Taleb et al. (1999) and gave some recommendations for some improvements in the analysis of progressive deformation rule by the design code RCC-MR.

There are several hardening rules available for ratchetting estimation. Each hardening rule has different advantages and disadvantages. Work done by Igari et al. (2002) for evaluation of thermal ratchetting due to moving temperature front, implementing different hardening rules, were reasonably conservative and established a fact that the prediction of the thermal ratchetting is strongly dependent on the constitutive model selected and completely accurate prediction of ratchetting strain is not always guaranteed by any of the models. Further, the implementation of hardening rules in FEM package is another difficulty in using Implicit/Explicit technique for plasticity integration. It is quite challenging for complex plasticity hardening to implement fully implicit technique into ABAQUS UMAT code used in present analysis. A simpler approach is used to implement a semi implicit scheme of plasticity integration where Newton's method is used to evaluate effective plastic strain increment implicitly. However, all other quantities (isotropic and kinematic hardening variable etc.) are updated explicitly.

2.1 Constitutive Model

Chaboche has suggested several constitutive models for time independent formulation such as inChaboche (1986), Chaboche and Rousselier (1983), Lemaitre and Chaboche (1990), Chaboche (1991). Present study involves combining hardening model of Chaboche and Rousselier (1983) for isotropic and kinematic hardening with normality hypothesis and associated flow rule obeying the von Mises yield criteria as below.

$$d\varepsilon^P = d\lambda \frac{\sigma' - X'}{J_2(\sigma - X)} \tag{1}$$

$$d\lambda = \frac{H(f)}{h} \left\langle \frac{3}{2} \frac{\sigma' - X'}{J_2(\sigma - X)} \right\rangle \tag{2}$$

$$J_2(\sigma - X) = \sqrt{\frac{3}{2}(\sigma - X) : (\sigma - X)} \tag{3}$$

$$f = J_2(\sigma - X) - R - k \tag{4}$$

$$h = C - \frac{3}{2}\gamma X \frac{\sigma' - X'}{J_2(\sigma - X)} + b(Q - R) \tag{5}$$

where $d\lambda$:plastic multiplier, σ' :deviatoric stress tensor, X' :deviatoric back stress tensor, X :back stress, $J_2(\sigma - X)$:the second invariant of the deviatoric stresses, R :drag stress in isotropic harde-

ning, P :accumulated plastic strain, $d\varepsilon^P$:plastic strain increment, f :yield function, h :hardening modulus (i.e. the value of $d\sigma / d\varepsilon^P$), $H(f)$:Heaviside step function, k :initial yield stress. $\langle \bullet \rangle$ is Macaulay's bracket which means that, $\langle x \rangle = 0$ for $x \leq 0$ and $\langle x \rangle = x$ for $x > 0$.

The rate of change of back stress describing kinematic hardening is given by:

$$\dot{X} = \frac{2}{3} C d\varepsilon^P - \gamma X \dot{P} \tag{6}$$

where C, γ :material parameters defining kinematic hardening, $\dot{P}$: accumulated plastic strain rate. The evolution of isotropic hardening variable is given by:

$$\dot{R} = b(Q - R)\dot{P} \tag{7}$$

where Q is asymptotic value which corresponds to a regime of stabilized cycles and b indicates the speed of stabilization. Work done by Lee et al. (2003) regarding material behavior and their properties describing kinematic and isotropic hardening as given in Table 1 have been extensively used as reference for the present study.

Parameters	Value
C(MPa)	92400
Γ	1390
B	14.6
Q(MPa)	51.1
k(MPa)	59.4

Table 1: Material constants.

2.2 Implicit plastic integration formulation

The analysis is performed with the concept of radial return technique introduced in Crisfield (2000) to ensure the unconditional stability during plastic deformation. Newton's method (Implicit scheme) of integration for effective plastic strain increment is used while all other quantities are integrated explicitly with self-developed FORTRAN coding. In implicit scheme, momentum balance or equilibrium equations require the determination of Jacobian that comprises the tangent stiffness matrix and load stiffness matrix. Since the tangent stiffness matrix is dependent on material behaviour hence constitutive model chosen for material behaviour should be realistic so as to give accurate results for strain calculation. Incremental plastic strain can be evaluated by applying the consistency condition for the von Mises yield criteria discussed in Dunne and Petrinic (2004), as follows:

$$df(\sigma, P) = \frac{\partial f}{\partial \sigma} : d\sigma + \frac{\partial f}{\partial P} dP \tag{8}$$

$$d\Delta P = \frac{f}{3G + A_i^{'} + A_k^{'}} \tag{9}$$

Where $A_i^{'}$ and $A_k^{'}$ are hardening parameters representing the derivative of isotropic hardening variable with respect to effective plastic strain increment ($\partial R / \partial \Delta P$) and the derivative of effective

trial stress with respect to plastic strain increment ($\partial\sigma_e^{tr}/\partial\Delta P$) respectively. σ_e^{tr} is the equivalent von Mises stress defined by equation (3) following J_2 flow theory. ΔP is the effective plastic strain increment which needs to be updated at every iteration. Nonlinear isotropic and kinematic hardening variables are updated from (t) to $(t+1)^{th}$ increment as follows:

$$R_{(t+1)} = R_{(t)} + \Delta R \tag{10}$$

$$X_{(t+1)} = X_{(t)} + \triangle X \tag{11}$$

3 THERMAL RATCHETTING ANALYSIS

Progressive inelastic deformation produced due to cyclic thermal loading along the axis of thin cylindrical shell can cause contraction or expansion depending upon loading conditions and geometry of the specimen. Further, the loading also affects the elastic-plastic behaviour of the structure such that the structure achieves the steady state of plastic straining called as shakedown and fails due to low cycle fatigue. Alternatively, if the structure undergoes progressive deformation such that there is increase in plastic strain cycle by cycle, the structure collapses after gross plastic deformation which is known as ratchetting.

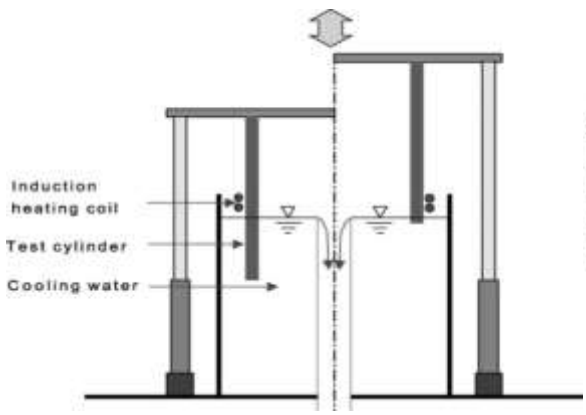

Figure 2: Schematic of experimental setup for ratchetting by Lee et al. (2003).

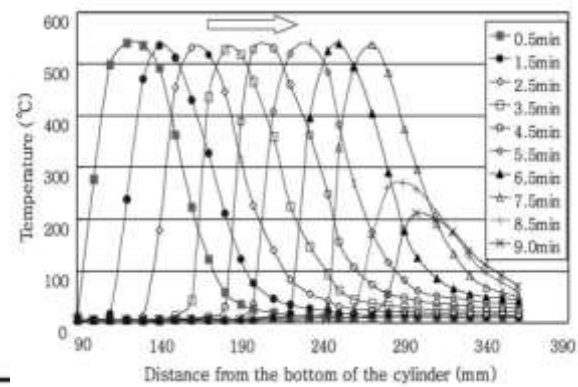

Figure 3: Transient temperature profile measured by thermocouples as per Lee et al. (2003).

In order to illustrate the shakedown and thermal ratchetting deformation due to cyclic thermal loading caused by free level variations in sodium pool, let us consider the work done by Lee et al. (2003), in which thin cylindrical shell of SS-316 L was examined for nine cycles of thermal loading. However, the Abdel-Karim (2005) review study shows that nine loading cycles are not sufficient to recognize whether shakedown occurs or progressive ratchetting will take place. In this context two cases, Case-A and Case-B are discussed in following sections to show shakedown and ratchetting of the structure (thin hollow cylindrical shell), by applying different loading methods for Case-A and Case-B. Case-A has two parts, been the first the validation of the code developed for predicting progressive deformation, while the second highlights shakedown behaviour. Case-B is investigated by imposing thermal load (induction heating) to the cylinder that is moving up and down into the pool.

Finite Element Model

Analysis in Case-A and Case-B are done for a cylinder of 600 mm outer diameter (OD), height 500 mm and 3 mm thickness, using a FEM model with 600 axisymmetric four noded quadratic elements.

Figure 2 shows the schematic diagram of the thermal ratchetting experimental setup as per Lee et al. (2003), to simulate axial movement of temperature distribution. The loading method applied in Case-B is used to simulate sodium free level variations for small travelling distance in $1/25^{th}$ scaled down model of the Prototype Fast Breeder Reactor (PFBR) main vessel (assumed smooth). This analysis is performed in Section 3.3, considering a cylinder of 500 mm OD, 600 mm height and 1 mm thickness, using an axisymmetric FEM model of 1714 four noded quadratic elements. As a boundary condition, the top surface is fixed in the axial direction throughout the analysis performed in the present study.

3.1 Case-A: The test cylinder was heated only when moving down into the pool.

a) Thermal loading condition

A smooth thin hollow cylinder of 600mm (OD), height 500 mm and 3 mm thickness is analyzed in ABAQUS by imposing nine cycles of thermal loading as shown in Figure 3, so as to validate the coding implemented in UMAT subroutine. This case of loading simulates the up and down movement of the thin hollow cylinder in a water filled container with fixed induction heating coil, being the cylinder heated when it is moving down into the water.

The evaluation of progressive inelastic strain due to level variation has been computed by introducing user defined subroutine incorporated in the finite element package. It includes FILM subroutine to take care of time dependent temperature and heat transfer properties and material subroutine UMAT. The material subroutine is formulated such that it will take care of Isotropic hardening and Kinematic hardening behaviour of material following Chaboche combined hardening model.

Residual radial displacement

The progressive inelastic deformation at the end of each cycle is measured for nine loading cycles and it is recorded for 150 mm of level variations. The displacements after three cycles and nine cycles are -0.98 mm and -2.57 mm respectively (-ve sign is for radially outward displacement). Figure 4 and Figure 5 shows the residual radial displacements after the 3^{rd} and the 9^{th} cycle, respectively. Both figures compare the results of the experimental test and the analysis performed for nine cycles, by Lee et al. (2003), with the results obtained with the present analysis. The values obtained here by semi implicit plastic integration, as discussed by Dunne and Petrinic (2004), are reasonably close to the ones obtained for the experimental structural test with nine cycles. The present analysis result for nine cycles is found to be in reasonable agreement to 1.79 mm as experimental value, and 2.74 mm as the analysis value obtained by Lee et al. (2003). Slight shift in location of peak displacement is observed from the superimposed plots. However the value of displacement in the radial direction is a matter of concern for ratchetting analysis, since ratchetting strain limit is 1% for base

metal and 0.5% for weld metal as per RCC-MR (1993) so the observed difference in location of peak displacement can be ignored.

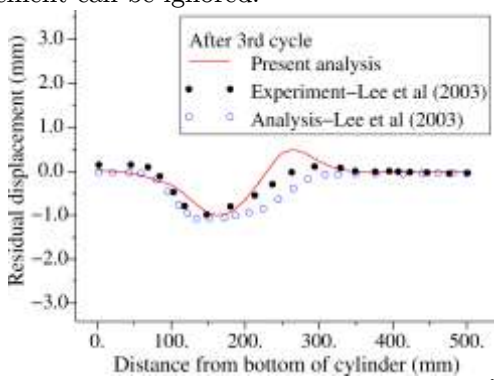

Figure 4: Comparison of residual displacement after 3rd cycle.

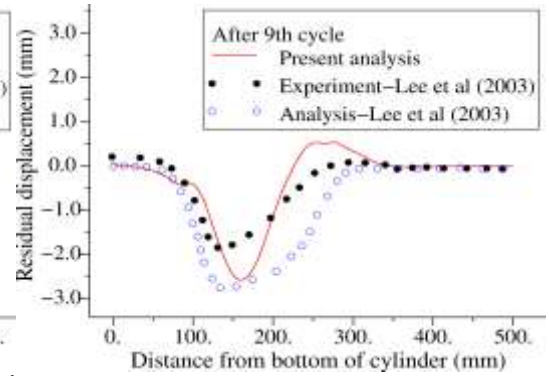

Figure 5: Comparison of residual displacement after 9th cycle.

b) Thermal loading condition

Thermal loading similar to that as mentioned in the Case-A is applied for fifteen cycles and the displacement is recorded cycle by cycle to recognize the phenomenon of shakedown. ABAQUS FILM subroutine is formulated so as to produce cyclic temperature variation at the curved surface of cylinder by imposing moving temperature profile along the axis of cylinder. Temperature profile can be generated by varying the film coefficient along the axis of cylinder. Film coefficients considered for water is 1100 W/m^2 K while that of heater is 800 W/m^2 K. The rate of change of the film coefficient with respect to the surface temperature is kept equal to zero.

Residual radial displacement leading to shakedown

The analysis is done for fifteen no. of cycles to study the progressive inelastic strain accumulation. The observation leads to the residual radial displacement of -3.2 mm (radially outwards) at the end of 15th cycle. Residual radial displacement in outward direction (i.e. expansion) cycle by cycle is shown in Figure 6 for 9th cycle up to 15th. Buckling is also noted in the present analysis at some locations of the cylinder, since outward radial displacement is exceeding the thickness value of the cylinder considered.

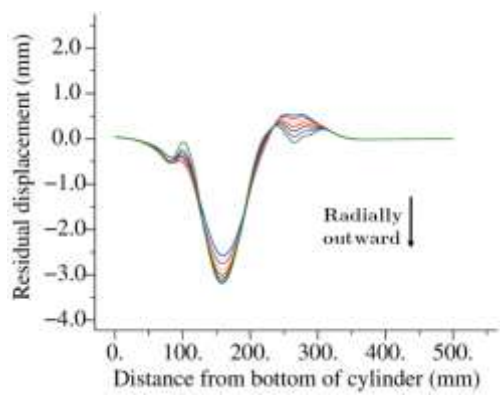

Figure 6: Profile of residual radial displacements in outward direction (after 9thcycle upto 15th cycle).

3.2 Case-B: The test cylinder was heated when moving up and down into the pool.

Thermal loading condition

Thermal loading as in Case-A is applied such that thermal gradient ($\Delta T/\Delta Z$) along the axis of the cylinder is the same during up and down movement of the cylinder. Figure 7 shows the transient thermal loading at different instances of time.

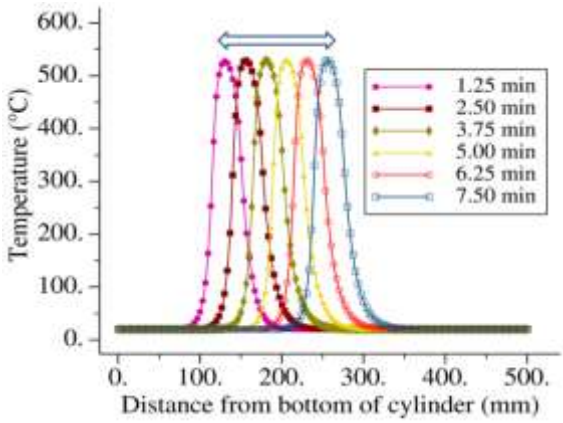

Figure 7: Temperature distribution along the axis of cylinder.

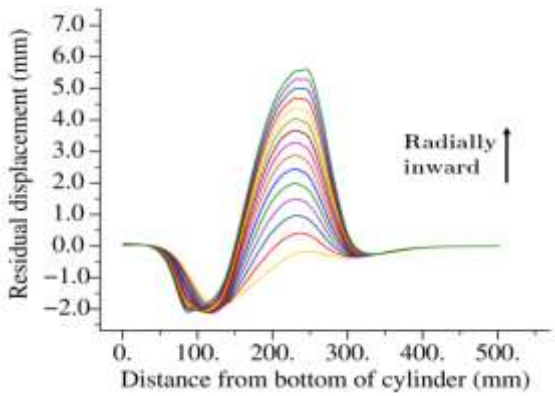

Figure 8: Profile of residual radial displacements in inward direction (for 15 cycles).

Residual radial displacement (ratchetting)

The analysis is done for fifteen no. of cycles to study the progressive inelastic strain accumulation. Residual displacements are recorded cycle by cycle as shown in Figure 8. The cyclic thermal loading due to level variations leads to the residual radial displacement of 5.6 mm (radially inwards) at the end of 15^{th} cycle. Figure 8 shows ratchetting with slow rate of decrease in progressive deformation which may lead to infinite ratchetting as discussed by Hubel (1996) and may collapse due to excessive deformation after large number of cycles. From the plot it can be inferred that deformation mode from expansion to contraction also depends on the loading method apart from geometry and travelling speed of temperature gradient as per Lee et al. (2003). Expansion in the first few cycles is observed while the cylinder contraction mode of deformation dominates and net inward deformation is finally observed in this case of loading method.

3.3 Ratchetting analysis in main vessel of PFBR

Cylinder with a height of 600 mm, OD 500 mm and thickness of 1 mm will simulate $1/25^{th}$ scale down model of the main vessel for the PFBR for thermal ratchetting. Thermal loading as applied in this section will simulate the upward and downward movement of the cylinder specimen in water filled container with the help of stepper motor. Induction heater is used to locally heat the cylinder continuously. Temperature distribution along the axis of the cylinder is considered to travel a distance of 50 mm of the centre portion of cylindrical shell, instead of long travelling distance of 150 mm as in Case-A.

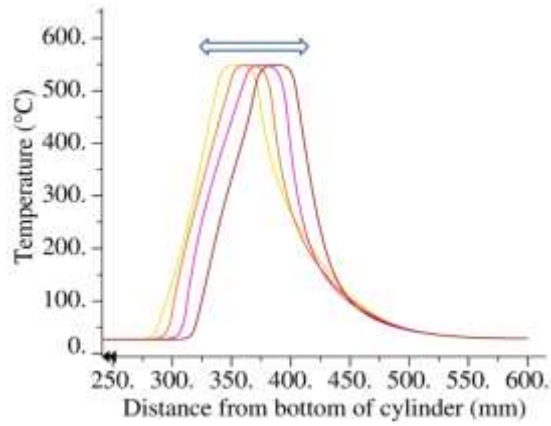

Figure 9: Temperature distribution along the axis of cylinder at different time instances of 40 seconds.

Thermal loading condition

Thermal loading is imposed using user defined FILM subroutine which takes care of the temperature variation along the surface of the cylinder. The temperature of about 550 °C is imposed. The typical temperature variation along the inner surface of the cylinder at different time instances of 40 seconds is shown in Figure 9. Temperature profile move with a speed of 0.31 mm/s. Range of horizontal axis in Figure 9 (i.e. Distance from bottom of cylinder) is 250 mm to 600 mm so as to represent the region of level variations clearly.

Residual radial displacement

The value of residual radial displacement of the inner surface of the cylinder is plotted against axial coordinate of the cylinder, at the end of each cycle. Range of horizontal axis in Figure 10 (i.e. Distance from bottom of cylinder) is 300 mm to 440 mm so as to represent the region of radial deformation clearly. Figure 10 shows a maximum displacement of -0.75mm (radially outward) at the position of 367.5 mm while maximum inward displacement is 0.17 mm at 405 mm.

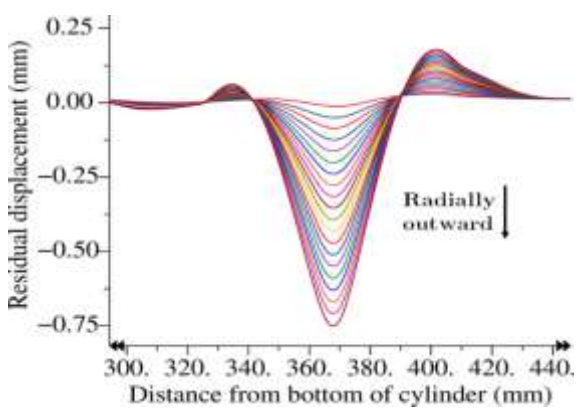

Figure 10: Profile of residual displacements (for 20 cycles).

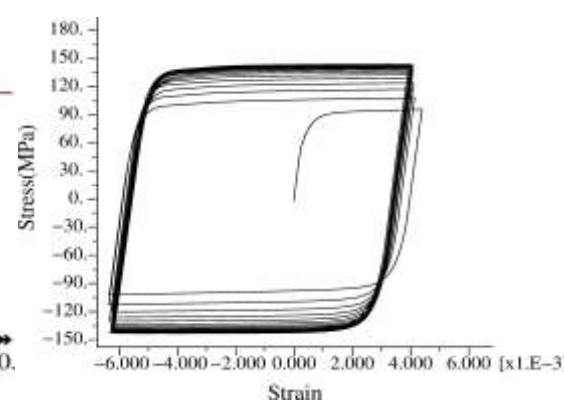

Figure 11: Stress-Strain hysteresis loop at 325 mm from bottom of cylinder.

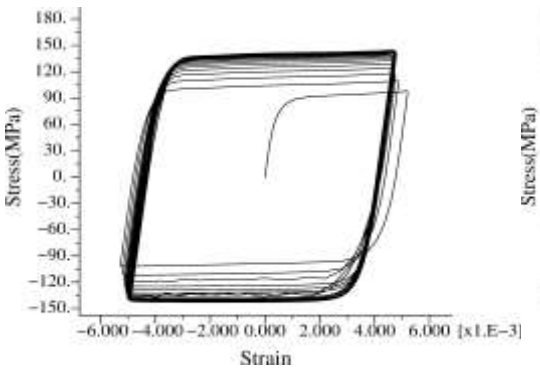

Figure 12: Stress-Strain hysteresis loop at 345 mm from bottom of cylinder.

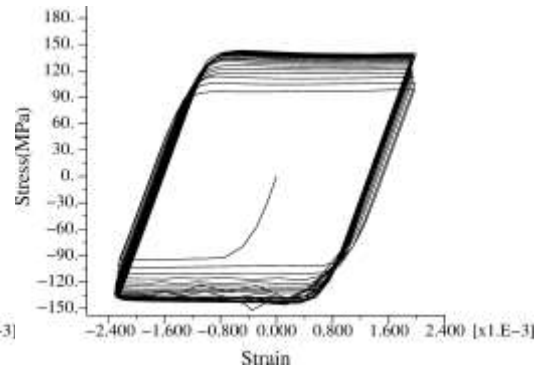

Figure 13: Stress-Strain hysteresis loop at 390 mm from bottom of cylinder.

Hoop Strain

The progressive inelastic ratchetting strain is very important in the circumferential direction because excessive deformation beyond acceptable limit can cause dimensional instability. The positions corresponding to the transition region of changing the mode of contraction to expansion or vice-versa is identified and the nodal position at 325 mm, 345 mm and 390 mm from bottom of cylinder are considered to evaluate hoop strain. Stress-strain hysteresis loop at different nodal position of high von Mises stress is shown in Figure 11, Figure 12 and Figure 13. The above nodal positions achieved saturation after few no. of cyclic loading. The saturated stress-strain curve shown here, establish the fact that radial deformation is bounded by these saturated regions along the axis of cylinder.

4 RESULTS

Results for Case-A & Case-B are compared here with the help of a plot between residual radial displacement and no. of ratchet cycles. The total residual strain accumulated at the end of nine cycles due to cyclic thermal loading is recorded and outward radial displacement of 2.57 mm in the cylinder can be seen in the Figure 14. The recorded value of the present analysis is an improvement and in reasonable agreement with 1.79 mm as experimental value, and 2.74 mm as the value of inelastic analysis in ABAQUS obtained by Lee et al. (2003). Further, the analysis is continued to recognize total number of loading cycles required to bring shakedown state. Fifteen no. of load cycles in Case-A is required to notice shakedown. Observation leads to the rapid saturating behaviour of the curve. Total outward radial displacement after fifteen no. of cycles is estimated to be 3.2 mm. Case-B in Figure 14 shows slow saturating behaviour of material compared to Case-A. Change in deformation mode from expansion to contraction is also observed. Total inward radial displacement after fifteen no. of cycles is estimated to be 5.6 mm.

In Section 3.3, scaled down model of PFBR is investigated for predicting ratchetting strain incorporating Chaboche model for combined isotropic and kinematic hardening. The plot between residual displacement and no. of ratchet cycles (Figure 15) still shows strain accumulation at an approximately constant rate and not getting saturated to attain finite ratchet strain value at the end of twenty loading cycles. It can be inferred from this analysis that the cylinder deformation is not reaching stable conditions and it may lead to progressive ratchetting instead of shakedown.

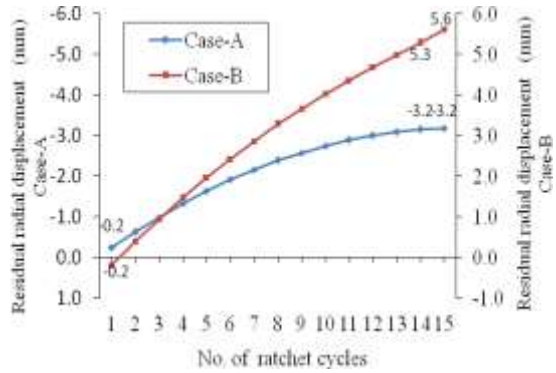

Figure 14: Comparison of residual displacement for Case A (radially outward) and Case B (radially inward).

Radial displacement at a critical location of maximum deformation is plotted against time in Figure 16 to show the progressive increase in radius. The estimated value of residual radial displacement after twenty cycles is -0.75 mm (-ve sign for radially outward displacement). For greater no. of cycles, the progressive deformation can be easily estimated by the extrapolation method available in RCC-MR Appendix A10 as discussed in the previous work by Cabrillat et al. (1993) and Chellapandi et al. (2000). The equation for extrapolation method is reproduced here.

$$\varepsilon_N = \varepsilon_n + (\delta\varepsilon_n/(m-1)) * [1 - 4^{1-m}] + (\delta\varepsilon_n / 4^m) * [N - 4n] \tag{12}$$

where N = Total number of imposed cycles

n = Number of load cycles analyzed

ε_n = Strain predicted at end of 'n' th cycle

ε_{n-1} = Strain predicted at end of 'n-1' th cycle

ε_{n-2} = Strain predicted at end of 'n-2' th cycle

$\delta\varepsilon_n$ = $\varepsilon_n - \varepsilon_{n-1}$: $\delta\varepsilon_{n-1} = \varepsilon_{n-1} - \varepsilon_{n-2}$: $\delta\varepsilon_{n-2} = \varepsilon_{n-2} - \varepsilon_{n-3}$

m_1 = $\log(\delta\varepsilon_n / \delta\varepsilon_{n-1}) / \log((n-1)/n)$

m_2 = $\log(\delta\varepsilon_n / \delta\varepsilon_{n-2}) / \log((n-2)/n)$

m_3 = $\log(\delta\varepsilon_n / \delta\varepsilon_{n-3}) / \log((n-3)/n)$

m = $0.9 \times \min(m_1, m_2, m_3)$

Based on the above equation, the extrapolated value for twenty cycles is first evaluated and compared with the results obtained in section 3.3 by taking the value of deformations in first five cycles. The radial displacements (mm) at the end of 1st, 2nd, 3rd, 4th and 5th cycles are -0.012, -0.05, -0.086, -0.125 and -0.162 respectively.

Value predicted by applying equation (12) for radial growth is -0.74 mm for 20 cycles which closely matches with the Abaqus analysis result of -0.75 mm obtained for 20 cycles.

The above procedure is then applied to evaluate the total accumulated strain after 50 cycles of loading. A value of 1.90 mm of radial displacement is predicted for the temperature difference of 550 °C. The temperature difference in PFBR sodium pool is about 200 °C. Hence the value of displacement due to accumulated ratchetting strain will be 0.69 mm which can be scaled up to PFBR main vessel resulting into 17.25 mm (radially outward).

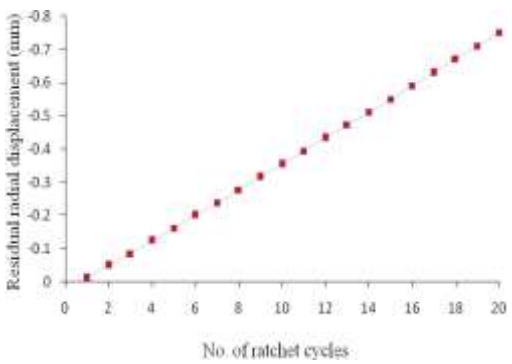

Figure 15: Ratchetting deformation with increase in no. of cycles.

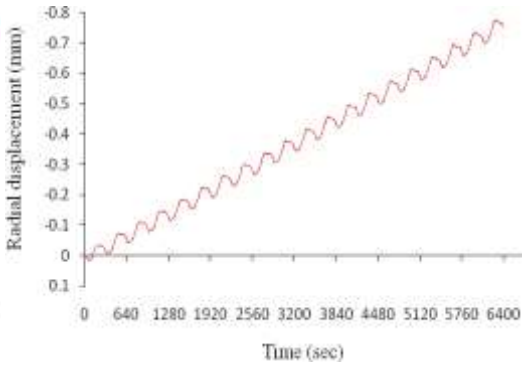

Figure 16: Radial displacement (outward direction) with time.

5 CONCLUSION

Shakedown and ratchetting studies of thin hollow cylindrical shell have been carried out using self-developed UMAT subroutine in ABAQUS. To establish the shakedown, number of loading cycles has been increased, which has been presented in Case-A, subsection (b). Figure 14 shows the curve for Case-A has attained its saturated value, i.e. -3.2 mm at the end of 14^{th} cycle and remained the same in the next cycle. Thus, pessimistically it can be said that after 15 cycles the shakedown is attained.

The deformation pattern changes with respect to the variation in loading method as presented in Case-B, where inward deformation of cylinder is noted compared to outward deformation in Case-A. Case-B in Figure 14 shows that the curve has attained 5.3 mm and 5.6 mm at the end of 14^{th} cycle and 15^{th} cycle respectively. At the end of the 15^{th} cycle, geometrical thinning is observed in the region of maximum radial deformation.

Ratchetting strain is calculated for $1/25^{th}$ scale down model of the PFBR main vessel with simplified thermal loading. The estimated radial displacement at the end of 50 cycles is 17.25 mm (outward), which is less than PFBR main vessel thickness (25 mm), so there is no problem for buckling risk as per the present analysis.

The analysis indicated that SS 316 L material exhibits combined isotropic and kinematic hardening. Considering only combined isotropic and kinematic hardening lead to overestimation of accumulated deformation, which can be reduced by using appropriate integration technique. Referring to Lee's work, ABAQUS result for maximum residual radial displacement after 9^{th} cycle was 2.74 mm and experimental result was 1.79 mm, which shows overestimation of radial displacement. In present analysis this overestimation is slightly reduced to 2.57 mm by using semi-implicit integration technique approaching the experimental value. To ensure the functional limit, the resulting deformation should not introduce any constraints for the free movement of inspection equipment which scans the outer surface of main vessel. Hence realistic constitutive model should be developed and employed to improve progressive deformation prediction capability so as to limit the radial deformations within acceptable range, considering actual thermal loading of PFBR, visco-plasticity, age-hardening, time-recovery and creep, which will be done in future.

ACKNOWLEDGEMENTS

The authors would like to express sincere thanks to Dr. Hyeong-Yeon Lee for his helpful comments and support.

References

ABAQUS version 6.10., (2010). Dassault Systèmes Simulia Corp., Providence, RI, USA.

Abdel-Karim, M., (2005). Shakedown of complex structures according to various hardening rules. International Journal of Pressure Vessels and Piping 82(6): 427–458.

ASME, (1995), Section III, Division 1- Subsection NH. Class 1 Components in elevated temperature services.

Bree, J., (1967). Elastic–plastic behaviour of thin tubes subjected to internal pressure and intermittent high-heat fluxes with application to fast nuclear reactor fuel element. Journal of Strain Analysis for Engineering Design 2 (3): 226-238.

Cabrillat, MT., Gatt, JM., (1993). Evaluation of thermal ratchetting on axisymmetric thin shells at the free level of sodium-Inelastic Analysis. Transactions of the 12th International Conference on Structural Mechanics in Reactor Technology (SMIRT), E05-4: 155-159.

Chaboche, JL., (1986). Time-independent constitutive theories for cyclic plasticity. International Journal of Plasticity 2 (2): 149-188.

Chaboche, JL., (1991). On some modifications of kinematic hardening to improve the description of ratchetting effects. International Journal of Plasticity 7(7): 661-678.

Chaboche, JL., (1994). Modelling of ratchetting: evaluation of various approaches. European Journal of Mechanics Part A: Solids 13: 501-518.

Chaboche, JL., Rousselier, G., (1983). On the plastic and viscoplastic constitutive equations. Part I. Rules developed with internal variable concept. Journal of Pressure Vessel Technology 105(2): 153-158.

Chaboche, JL., Rousselier, G., (1983). On the plastic and viscoplastic constitutive equations. Part II. Application of internal variable concept to the 316 stainless steel. Journal of Pressure Vessel Technology 105(2): 159-164.

Chellapandi, P., Chetal, SC., Bhoje, SB., (2000). Theoretical and experimental simulation of thermal ratchetting of thin vessels in PFBR. Transactions of the Indian Institute of Metals 53(3): 391-399.

Crisfield, MA., (2000). Non-linear Finite Element Analysis of Solids and Structures. Vol-2, John Wiley Sons (New York).

DDS, (1998). Demonstration fast breeder reactor high temperature structure design rules. The Japan Atomic Power Company.

Dunne, F. and Petrinic, N., (2004). Introduction to Computational Plasticity, Oxford University Press (UK).

Hubel, H., (1996). Basic conditions for material and structural ratcheting. Nuclear Engineering and design 162(1): 55-65.

Igari, T., Wada, H., Ueta, M., (2000). Mechanism-based evaluation of thermal ratchetting due to travelling temperature distribution. Journal of Pressure Vessel Technology 122(2):130-138.

Igari, T., Kobayashi, M., Yoshida, F., Imatani, S., Inoue, T., (2002). Inelastic analysis of new thermal ratchetting due to a moving temperature front. International Journal of Plasticity 18(9): 1191–1217.

Lee, HY., Kim, JB., Lee, JH., (2003). Thermal ratchetting deformation of a 316L stainless steel cylindrical structure under an axial moving temperature distribution. International Journal of Pressure Vessels and Piping 80(1): 41–48.

Lemaitre,J. and Chaboche, JL., (1990). Mechanics of solid materials, Cambridge University Press (Cambridge).

RCC-MR (1993). Regles de conception et construction des materiels mecaniques des iots nucleaires RNR, AFCEN, Paris.

Taleb, L., Cousin, M., Cabrillat, MT., Galineau, O., Waeckel, N., (1999). Comparison between simplified predictive methods of the ratchetting phenomenon. Transactions of the 15th International Conference on Structural Mechanics in Reactor Technology (SMIRT), F03-5: 121-128.

Wada, H., Odani, T., Fujioka, T., (1997). The ratchetting evaluation methods in Japanese demonstration FBR design. Transactions of the 14th International Conference on Structural Mechanics in Reactor Technology (SMIRT), F04-2: 85-92.